Environmental Science & Technology

Article

pubs.acs.org/est

Cellular Internalization of Dissolved Cobalt Ions from Ingested $CoFe_2O_4$ Nanoparticles: In Vivo Experimental Evidence

Sara Novak,[†] Damjana Drobne,[†,‡,§,*] Miha Golobič,[†] Jernej Zupanc,[†] Tea Romih,[†] Alessandra Gianoncelli,[∥] Maya Kiskinova,[∥] Burkhard Kaulich,[∥] Primož Pelicon,[⊥] Primož Vavpetič,[⊥] Luka Jeromel,[⊥] Nina Ogrinc,[⊥,▽] and Darko Makovec[#]

[†]Department of Biology, Biotechnical Faculty, University of Ljubljana, Večna pot 111, 1000 Ljubljana, Slovenia

[‡]Centre of Excellence, Advanced Materials and Technologies for the Future (CO NAMASTE), Jamova cesta 39, 1000 Ljubljana, Slovenia

[§]Center of Exelence, Nanoscience and Nanotechnology (Nanocentre), Jamova cesta 39, 1000 Ljubljana, Slovenia

[∥]Elettra-Sinchrotrone Trieste S.C.p.A., Strada Statale 14-km 163.5 in AREA Science Park, 34149 Basovizza, Trieste, Italy

[⊥]Jožef Stefan Institute, Microanalytical Center, Department for Low and Medium Energy Physics, Jamova cesta 39, 1000 Ljubljana, Slovenia

[#]Institute Jozef Stefan, Jamova cesta 39, 1000 Ljubljana, Slovenia

[▽]LOTRIC Metrology, Selca 163, 4227 Selca, Slovenia

Supporting Information

ABSTRACT: With a model invertebrate animal, we have assessed the fate of magnetic nanoparticles in biologically relevant media, i.e., digestive juices. The toxic potential and the internalization of such nanoparticles by nontarget cells were also examined. The aim of this study was to provide experimental evidence on the formation of Co^{2+}, Fe^{2+}, and Fe^{3+} ions from $CoFe_2O_4$ nanoparticles in the digestive juices of a model organism. Standard toxicological parameters were assessed. Cell membrane stability was tested with a modified method for measurement of its quality. Proton-induced X-ray emission and low energy synchrotron radiation X-ray fluorescence were used to study internalization and distribution of Co and Fe. Co^{2+} ions were found to be more toxic than nanoparticles. We confirmed that Co^{2+} ions accumulate in the hepatopancreas, but Fe^{n+} ions or $CoFe_2O_4$ nanoparticles are not retained in vivo. A model biological system with a terrestrial isopod is suited to studies of the potential dissolution of ions and other products from metal-containing nanoparticles in biologically complex media.

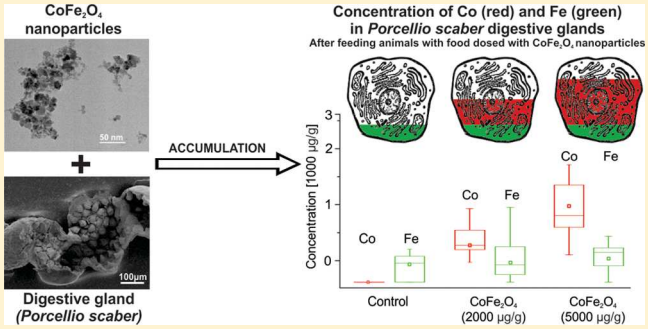

INTRODUCTION

In the past decade, magnetic nanoparticles (NPs) have attracted much attention because of their potential use in different fields such as medicine, electronics, and energetics.[1−8]

Because of increased use in many fields, high concentrations of $CoFe_2O_4$ NPs in industrial wastewaters and surrounding soils can occur and negatively affect humans and the environment. One of the important issues which must be resolved before $CoFe_2O_4$ nanoparticles can be widely used and safely controlled refers to dissolution of cobalt (Co) from $CoFe_2O_4$ nanoparticles. Cobalt ions (Co^{2+}) may induce the formation of Reactive Oxygen Species (ROS),[9] oxidize proteins,[10] and cause oxidative DNA damage.[11] Consequently, the possible dissolution of the cobalt ions from $CoFe_2O_4$ particles must be controlled.

It is now widely recognized that such dissolution plays an important role in nanoparticle toxicity, but the reach of this phenomenon remains unclear. It has been found to be influenced mainly by pH but also by the specific surface area of the nanoparticles.[12] Natural organic compounds in the cellular media may either enhance or reduce the release of ions from nanoparticles, depending on their chemical composition and concentration.[12,13]

Methods used for studying dissolution include different chemical analytical methods, such as atomic absorption spectroscopy (AAS),[14] inductively coupled plasma mass spectrometry (ICP-MS),[15] and localized surface plasmon resonance (LSPR).[16] These methods may be used in conjunction with ultracentrifugation of a suspension that

Received: December 24, 2012
Revised: March 29, 2013
Accepted: April 11, 2013
Published: April 11, 2013

   dx.doi.org/10.1021/es305132g | Environ. Sci. Technol. 2013, 47, 5400−5408

Table 1. Parameters of Experiments[a]

	experiment A	experiment B	experiment C	experiment D
$CoFe_2O_4$ NPs concentration	1000	2000	1000	2000
on leaves (μg/g leaf)	2000	/	2000	5000
$CoCl_2$ concentration on	1000	2000	/	2000
leaves (μg/g leaf)	2000	/	/	5000
number of animals in each exposure group	20	15	10	15
digestive gland membrane stability analyses (AO/EB)	+	+	+	−
tissue distribution of Co and Fe (PIXE)	+	−	−	−
cell distribution, colocalization of Co and Fe in gland cells (LE-XRF)	+	+	+	−
concentration of Co and Fe indigestive glands (AAS)	+	−	−	+

[a]Concentrations of tested substances, number of exposed animals per group and measured parameters in different experiments (+, parameters analyzed; −, parameters not analyzed).

separates the insoluble nanoparticles from ions that remain in solution.

Measurements of dissolved ions from particles in biological studies are useful only if they are conducted in biologically relevant media. As a rule, it is not possible to mimic biological media; therefore, it is necessary to conduct experiments in in vivo systems. Data on dissolution are very important to provide an insight into the potentially compromised efficiency of applied nanomaterials or their toxicity when coming in contact with biological fluids.

In the work presented here, we have selected a model biological system, in which $CoFe_2O_4$ nanoparticles are introduced via food. The digestive system of the terrestrial isopod *Porcellio scaber* is composed of a stomach, four blind-ending digestive gland tubes (hepatopancreas), and a gut. Food enters the digestive glands directly via the short stomach or after the reflux from the gut. In the hepatopancreas, the ingested material is mixed with digestive fluids. Measurements of pH in the gut of terrestrial isopods (*Porcellio scaber*) with a LIX-type pH microelectrode showed pH 5.5−6.0 in the anterior hindgut, and pH 6.0−6.5 in the posterior hindgut.[17] The pH value of the *P. scaber* digestive glands (hepatopancreas) is 6.1 ± 0.3 and at its distal region it is slightly more acidic, with a pH of 5.8−6.1.[18] This biological system is a complex biological environment which acts as an assembly of biologically relevant conditions that may affect dissolution of cobalt or iron ions from nanoparticulate $CoFe_2O_4$. When consumed particles entered the gut and digestive system, they are retained in the digestive system for 2−4 h. Reflux of partly digested food also reaches the digestive glands, but with some delay. Apart from digestion and absorption of food, one of the major roles of the digestive system is to accumulate metals in proportion to that in the gland lumen. In bioaccumulation studies with isopods, it is expected that accumulation of a metal is related to the bioavailable metal ion fraction of the gland fluid.[19,20]

The aim of this study was to provide experimental evidence on the formation of Co^{2+} and/or Fe^{2+}/Fe^{3+} ions from $CoFe_2O_4$ nanoparticles in the digestive juices of a model organism, accumulation of dissolved ions by digestive gland epithelium, cellular internalization of particles, as well as on their toxic potential. We hypothesize that metal ions are generated from ingested $CoFe_2O_4$ nanoparticles in a digestive system and that ions are accumulated by digestive gland cells proportional to exposure doses. We also hypothesize that if particles enter cells they may reach a location distinct from that occupied by ions that have been accumulated via other pathways.

MATERIALS AND METHODS

Chemicals. Acridine orange (AO), ethidium bromide (EB), sodium chloride (NaCl), potassium chloride (KCl), magnesium chloride ($MgCl_2$), glucose, and 2-amino-2-hydroxymethyl-propane-1,3-diol (TRIS), were purchased from Merck. Cobalt-(II) chloride hexahydrate ($CoCl_2 \cdot 6H_2O$), 99.9% (metal basis) was purchased from Alfa Aesar Johnson Mathey Company. $CoFe_2O_4$ nanoparticles were synthesized at the Department for Materials Synthesis, Jožef Stefan Institute in Ljubljana.

Model Organisms. Terrestrial isopods, *Porcellio scaber* (Isopoda, Crustacea), were collected in July, 2011 at an uncontaminated location near Ljubljana, Slovenia. The animals were kept in a terrarium filled with a layer of moistened soil and a thick layer of partly decomposed hazelnut tree leaves (*Corylus avellana*), at a temperature of 20 ± 2 °C and a 16:8 h light:dark photoperiod. Only adult animals of both sexes and weighing more than 30 mg were used. If moulting or the presence of marsupia were observed, then the animals were excluded from the experiment in order to keep the investigated population as physiologically homogeneous as possible.

Characterization of Nanoparticles. The nanoparticles were synthesized by coprecipitation using NaOH from aqueous solutions of Co(II) and Fe (III) ions at elevated temperatures.[21] The nanoparticle samples were thoroughly washed with water and then suspended in an aqueous solution of glucose. The suspended $CoFe_2O_4$ nanoparticles show strong agglomeration in distilled H_2O.

Nanoparticles were inspected with transmission electron microscopy (TEM) coupled with energy dispersive X-ray spectroscopy (EDXS) (JEOL 2010F) and the Zeta potential was also measured (Brookhaven Instruments Corp., Zeta-PALS). The aim of these analyses was to provide data on the suspension of particles and allow comparisons among different studies and within our experiments.

After exposure in feeding experiments, remnants of selected leaves were dried and attached to mounts with silver paint (SPI), gold−palladium sputtered (Sputter coater SCD 050, BAL-TEC), and investigated by field emission scanning electron microscopy (SEM) (Jeol JSM-6500F) at the Institute of Metals and Technology in Ljubljana. Energy dispersive X-ray analysis (EDX) was used to establish their chemical composition (EDS/WDS Oxford Instruments INCA, Jeol JSM-6500F) at the Institute of Metals and Technology.

Food Preparation. Hazelnut leaves were collected in an uncontaminated area and dried at room temperature and the animals consumed particles applied to a leaf surface. Dried leaves were cut into pieces of approximately 100 mg. The $CoCl_2$ or $CoFe_2O_4$ nanoparticles was suspended in distilled

water before each experiment to obtain final concentrations of cobalt of 1000, 2000, and 5000 μg/mL. To diminish agglomeration, a suspension of nanoparticles in H_2O was sonicated in an ultrasonic bath for 1 h and then immediately applied to the leaves.

In the control group, the leaves were treated with distilled water and in the test group, a suspension of particles was spread with a paintbrush onto the abaxial surface of leaves to give final nominal concentrations of 1000, 2000, and 5000 μg $CoCl_2$ or $CoFe_2O_4$ nanoparticles per gram (dry mass) of leaf. The leaves were allowed to stand until dry.

Experimental Procedure. Each individual animal was placed in a 9 cm Petri dish. One hazelnut leaf was treated with distilled water, or a suspension of $CoCl_2$ or nano-$CoFe_2O_4$ and placed in the dish as the animal's only food source. Humidity in the Petri dish was maintained by spraying tap water on the internal side of the lid every day. All Petri dishes were kept in a large glass container under controlled conditions in terms of air humidity (≥80%), temperature (21 ± 1 °C) and light regime (16:8 h light:dark photoperiod).

Different numbers of animals in each individual experiment were exposed to varying concentrations of nanoparticles for 14 days (Table 1). Four experiments, A, B, C, and D, were performed one at a time, and the exposure concentrations of suspensions and initial number of tested animals were selected on the basis of the type of analyses conducted after exposure.

The concentrations were chosen on the basis of our preliminary experiments. After exposure, the animals were anaesthetized at low temperature and then decapitated and their digestive glands isolated. In experiments, digestive gland tubes were used for different analyses (Table 1).

Feeding Parameters, Mass Change and Survival. After 14 days of exposure of the animals to treated leaves, faecal pellets and leaves were removed from the Petri dishes, dried at room temperature for 24 h, and weighed. The feeding rate of isopods was calculated as the mass of consumed leaves per wet mass of the animal per day. The food assimilation efficiency was calculated as the difference between the mass of consumed leaves and mass of faecal pellets divided by the mass of consumed leaf. The mass change of animals was determined as the difference in its mass from the beginning to the end of the experiment

AO/EB Analysis: Digestive Gland Cell Membrane Stability. Cell membrane stability was tested with a modified method for assessment of cell membrane stability, previously described by Valant et al.[22] In short, different permeability by the two dyes results in differentially stained nuclei as follows: Acridine orange is taken up by cells with membranes that are intact or destabilized, and the cell emits green fluorescence. Ethidium bromide on the other hand, is taken up only by cells with destabilized cell membranes, and such cells emit orange fluorescence, after intercalation into DNA.[23]

A single isolated hepatopancreatic tube was incubated for 5 min in a mixture of the fluorescent dyes acridine orange and ethidium bromide and then put on a microscope slide. Fresh samples were photographed and examined with an Axioimager Z1 fluorescent microscope (Zeiss) with two different sets of filters. The excitation filter 450 to 490 nm and the emission filter 515 nm (filter set 09) were used to visualize AO and EB stained nuclei, while the excitation filter 365 nm and the emission filter 397 nm (filter set 01) were used to visualize nuclei stained with EB only. Cell membrane integrity was assessed by examination of micrographs. Photographs of intact digestive glands were examined by the same observer twice at intervals of at least 24 h and cell membrane integrity was rated on the scale from 0 to 9 by visual inspection. On the basis of preliminary experiments, it was concluded that nontreated (control) animals showed <5% of nuclei stained by EB, while severely stressed animals have up to 100% of EB-stained nuclei. The <5% of hepatopancreatic tubes nuclei stained with EB were classified as 0, and those with the highest proportion (>95%) of EB stained nuclei as 9. [22]

Micro-PIXE Analysis: Tissue Distribution of Co and Fe. For microparticle induced X-ray emission (micro-PIXE) analysis, digestive glands were shock-frozen in liquid propane or N_2, using tissue-freezing medium (Jung Tissue Freezing Medium, Leica). Samples were sectioned with a section thickness of 60 μm using a Leica CM3050 cryotome (Leica) with the temperature of the microtome head and chamber maintained between −25 °C and −20 °C. The sections were placed in precooled Al holders, transferred to an alpha 2−4 Christ freeze-dryer using a cryo-transfer assembly cooled with liquid N_2, and then freeze-dried at −30 °C and 0.4 mbar for 24 h. Dry sections were mounted between two thin layers of Pioloform foil on the Al sample holder.[24,25]

For detection of X-rays between 1 and 25 keV, two X-ray detectors were used simultaneously. A high-purity germanium X-ray detector (active area 95 mm^2; beryllium window, 25-μm thick; polyimide absorber, 100 μm thick) positioned at 135° to the beam direction was used for the energy range of 4 keV-25 keV. Low energy X-rays in the range of 0.8−6 keV were detected by a Si(Li) detector (active area 10 mm^2) positioned at 125° to the beam direction. The proton dose was determined by a rotating in-beam chopper. Measurement of micro-PIXE emission and data evaluation for the biological samples of intermediate thickness at the micro-PIXE laboratory, previously described in detail,[24,26,27] was performed at the Jožef Stefan Institute in Ljubljana.

We analyzed cross sections of isolated digestive gland tubes from six animals. Two analyzed animals were control ones, two were fed on food dosed with 2000 μg/g with $CoCl_2$, and two animals on food dosed with 2000 μg/g nano-$CoFe_2O_4$. Two or three digestive gland tubes were isolated from each animal and analyzed.

LE-XRF Analysis: Cell Distribution and Colocalization of Co and Fe in Digestive Gland Cells. For Low Energy Synchrotron Radiation X-ray Fluorescence (LE-XRF) analysis, isolated digestive glands were shock-frozen in liquid N_2, using tissue-freezing medium (Jung Tissue Freezing Medium, Leica). Samples were sectioned with a section thickness of 14 μm using a Leica CM3050 cryotome (Leica) with the temperature of the microtome head and chamber maintained between −25 °C and −20 °C. The sections were placed in precooled Al holders, transferred to an alpha 2−4 Christ freeze-dryer using a cryo-transfer assembly cooled with liquid N_2, and then freeze-dried at −30 °C and 0.4 mbar for 24 h. Dry sections were mounted between two thin layers of Pioloform foil on the sample holder.

The LE-XRF experiments were carried out with the x-ray microscope TwinMic at the Elettra synchrotron radiation facility in Trieste[28,29] operating in the 400−2200 eV photon energy range. During the experiments, TwinMic was operated in STXM mode,[29] in which a microprobe is formed by a zone plate lens and the specimen is raster scanned across it. The TwinMic microscope can provide submicrometer spatial resolution, but we used a spot size and a step size of 1 μm,

which is a useful compromise between lateral resolution adequate for the features of interest and good XRF signal.

The STXM mode allows simultaneous acquisition of X-ray transmission (absorption and phase contrast images) and photon emission (XRF) signals.[30] The low X-ray energy range is particularly suited to biological investigations, and allows the simultaneous acquisition of the elemental distributions of elements of low atomic number (B to P) from the K emission lines and elements of higher atomic number (Ca to Nb) from the L emission lines. The absorption and phase contrast images are collected by a configurable detector arrangement consisting of a fast read-out electron multiplying CCD camera coupled to an X-ray-to-visible light conversion system. The LEXRF setup used for this experiment consists of an annular arrangement of 8 Si drift detectors (SDDs) (PNSensor, Munich, Germany), only 5 of which, coupled to read-out electronics, were used.[31,32] This arrangement currently allows only qualitative analyses. Full elemental quantification will be the subject of future reports.

The X-ray fluorescence spectra obtained for each pixel in the raster scan were batch processed by fitting the peaks with a Gaussian model and with a linear subtraction, using the PyMCA data analysis software.[33] Elemental maps were generated by plotting the intensity of the fluorescence peaks as a function of their position in the sample plane.

In experiment A (Table 1), a cross section of one isolated gland from a control animal, two isolated glands from one animal fed on food dosed with 2000 μg/g $CoCl_2$, and two sections of digestive gland tubes from one animal fed on food dosed with 2000 μg/g $CoFe_2O_4$ nanoparticles were analyzed. In experiment B, samples from one control animal and two sections from two animals from each treated group (animals fed on food dosed with 2000 μg/g $CoCl_2$ or $CoFe_2O_4$ nanoparticles) were analyzed. In experiment C, two sections from two different animals both fed on food dosed with 2000 μg/g nano-$CoFe_2O_4$ were analyzed. Altogether, 12 different cross-sections of digestive glands were analyzed.

AAS Analysis: Concentration of Co and Fe in Digestive Glands. Cobalt and iron were measured by atomic absorption spectroscopy in one or two isolated digestive gland tubes from each animal in experiments A and D. Prior to the analysis, samples were lyophilized, weighed, and completely digested in a 7:1 nitric acid/perchloric acid mixture. After evaporation of the acid, the residue was taken up in 0.2% HNO_3 and total Co and Fe concentrations in the digestive glands were determined by flame atomic absorption spectrometry (Perkin-Elmer AAnalyst 100) in the Department of Biology, University of Ljubljana. Within each measurement, certified reference material (TORT-2, National Research Council of Canada) was used to check the accuracy and precision of the analytical procedure. Along with the samples, 10 replicates of a known amount of certified reference material were also acid digested and each sample was measured in triplicate. Calculations followed the approach of Jorhem[34] and Phillips et al.[35] The certified concentration of Co in the reference material was 0.51 ± 0.09 mg/kg; our measurement was 0.64 ± 0.14 mg/kg (mean ± SD, n = 30); recovery was 125.5%, Z′ = 2.62. For Fe, the certified concentration in the reference material was 105 ± 13 mg/kg; our measurement was 101 ± 14 mg/kg (mean ± SD, n = 30); recovery was 96.2%, Z′ = −0.626.

Concentration of Co and Fe in the nano-$CoFe_2O_4$ Suspension Supernatant. For this analysis, suspensions of $CoFe_2O_4$ NPs and $CoCl_2$ in deionized water were prepared in the same way as that for the in vivo tests. The final concentrations were 2000 mg Co and 5000 mg Co/mL; each concentration was prepared in triplicate. The suspensions were ultracentrifuged twice at 100 000 g for 30 min at 20 °C. The supernatant was separated from the pellet formed by the nanoparticles and divided into two aliquots for further dilution. One aliquot was diluted with an equal volume of deionized water, the other one with an equal volume of 1 M HCl.[36] Then, a 3-mL portion from each aliquot was used for analysis by flame atomic absorption spectrometry (AAS, Perkin-Elmer Analyst 100). The difference in Co and Fe ion content between the acidified and nonacidified suspension indicates that nanoparticles remaining in the supernatant after centrifugation are dissolved. Measurement of $CoCl_2$ solution served as a check that centrifugation did not remove ions from the solution. Detection of Co and Fe by AAS is possible, provided that the concentrations of Co and Fe ions are above the detection limit (9 μg/L and 5 μg/L, respectively).

The original suspensions of $CoFe_2O_4$ NPs (2000 and 5000 mg/L of $CoFe_2O_4$) were also analyzed by AAS. Prior to the analysis the suspensions were diluted (1:1000 and 1:2500, respectively) with 1 M HCl and incubated in acid for 3 days to achieve complete dissolution.

Data Analysis. Data were analyzed by standard statistical methods. The difference in the median measured parameters in exposed and unexposed groups was tested with the nonparametric Mann−Whitney U test. All calculations were performed with Statgraphics Plus 4.0. Statistically significant differences between exposed and control animals were divided into three categories with different numbers of stars assigned (* $p < 0.05$, ** $p < 0.01$, *** $p < 0.001$).

RESULTS

Characterization of Nanoparticles. TEM analysis showed the nanoparticles to have a relatively broad size distribution between 5 and 15 nm (Figure S1A of the Supporting Information, SI). The smaller nanoparticles are globularly shaped; whereas the larger ones have an octahedral shape. Energy dispersive X-ray spectroscopy (EDS) analysis showed that their composition matched to stoichiometry of $CoFe_2O_4$. The size of the agglomerates of the nanoparticles on the surfaces of leaves in the experiments was between 1 and 10 μm (inspected with SEM, Figure S2 of the SI).

Zeta potential measurements showed the isoelectric point for $CoFe_2O_4$ nanoparticles at neutral pH. At pH 7.4, the zeta potential is slightly negative. SEM revealed that particles remained spread over the entire leaf surface (Figure S1B of the SI) and energy dispersive X-ray analysis (EDX) revealed their chemical composition (Table S1 of the SI).

Feeding Parameters, Mass Change and Mortality. Animals were exposed to leaves dosed with $CoCl_2$ or a suspension of $CoFe_2O_4$ NPs, providing nominal concentrations of 1000, 2000, or 5000 μg $CoCl_2$ or $CoFe_2O_4$ nanoparticles per g of leaf. Mass change and survival were not affected at these concentrators of $CoCl_2$ or nano-$CoFe_2O_4$ (Figures S3 and S4 of the SI). In all four experiments, there was a statistically significant difference in feeding rate between control groups and groups in which animals were exposed to 2000 or 5000 μg/g of $CoCl_2$. Exposure to $CoFe_2O_4$ nanoparticles had no effect on the feeding rate of animals in any experiment for the 14 days of the experiment. Compared to the control animals, the reduction in the feeding rate of animals exposed to $CoCl_2$ was

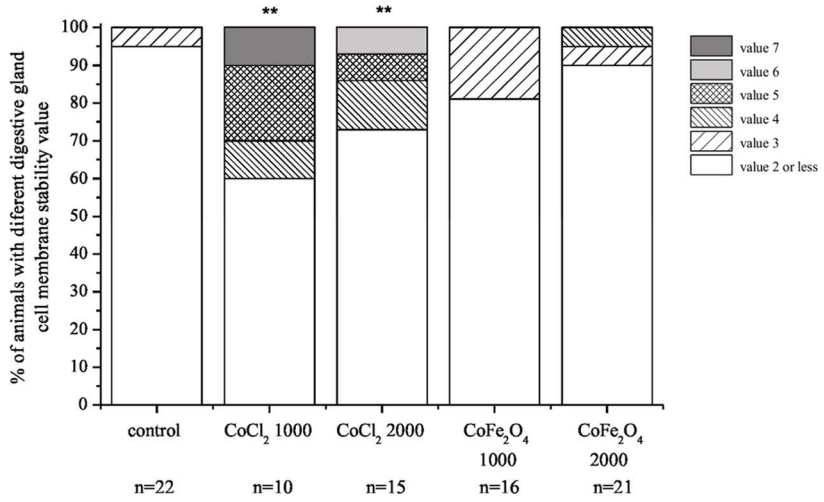

Figure 1. Percentage of animals in each exposure group in experiments A, B, and C with different degrees of destabilized cell membrane. Destabilization of the cell membrane was assessed visually and classified from 0 to 9 according to the predefined scale descibed in the Materials and Methods. Digestive gland cell membrane stability value of 2 or less denotes animals which did not have destabilized cell membranes and digestive gland cell membrane stability values from 3 to 9 animals with some degree of destabilization of the cell membranes. A value of 7 corresponds to the most highly destabilized cell membranes. Statistical significant differences between exposed and control animals are marked with ** ($p < 0.01$). Nominal exposure concentrations (1000 or 2000 μg $CoCl_2$ or nano-$CoFe_2O_4$/g of leaf) and number of animals per group (n) are provided on the x-axis.

statistically significant in higher concentrations (2000, 5000 μg/g) of Co in food as shown in Figure S5 of the SI).

AO/EB Analysis: Digestive Gland Cell Membrane Stability. Our previously published data demonstrate that the digestive gland cell membrane stability value was higher than 2 (on a scale from 0 to 9) in only 5% of animals from a stock culture and in good physiological condition, and this number was used as a benchmark.[22] The cell membranes are considered destabilized when this value is higher than 2.

We combine results on cell membrane stability from all three experiments (A, B, and C). The cell membrane stability of the controls was not affected in more than ~10% of the animals and this was considered to be normal. An exposure concentration of 1000 μg $CoCl_2$/g in the food caused digestive gland cell membrane destabilization in up to 40% of exposed animals and an exposure concentration of 2000 μg $CoCl_2$/g in the food caused destabilization in up to 30% of exposed animals. Upon exposure to 1000 or 2000 μg nano-$CoFe_2O_4$ per g dry mass of leaves, approximately 10% and 20% of exposed animals, respectively, had destabilized digestive cell membranes. This is not statistically significantly different from the controls, where one animal out of 22 had a destabilized cell membrane. The highest proportion of animals with destabilized membranes was found in a group fed on food containing 1000 μg $CoCl_2$/g dry mass of leaf. There was no statistical difference between a group of animals fed on food containing 1000 μg $CoCl_2$/g dry mass of leaf and a group of animals fed with 2000 μg $CoCl_2$/g dry mass of leaf (Figure 1).

Micro-PIXE Analysis: Tissue Distribution of Co and Fe. In the micro-PIXE analysis, the concentrations of elements with values above Minimum Limits of Detection (MLDs) are simultaneously analyzed. In parallel to the distribution of Co and Fe in the tissue, the distribution of Cu is determined, indicating the locations of metal storing granules in the S-cells of the digestive gland epithelium.

In all of the samples analyzed, the concentrations of Fe were similar. In all of the animals exposed to food dosed with $CoFe_2O_4$ NPs, concentrations of Co were statistically significantly higher than those measured in controls, where in most cases Co was below limit of detection (Figure 2A). As expected, very high concentrations of Co were also detected in animals fed with $CoCl_2$-dosed food (Figure 2B). Overlap with Cu was observed (Figure 2B,C) in all cases where Co was found in the epithelium. This colocalization indicates that Co, either originating from $CoCl_2$ or from nano-$CoFe_2O_4$, is stored in metal-storing granules of S-cells. LE-XRF was used to assess colocalization of Co and Fe in the gland epithelium. This provides better spatial resolution (1 μm) allowing analysis at subcellular length scales. The same XRF protocol has been used successfully to analyze cellular distribution and degradation of $CoFe_2O_4$ NPs in fibroblast cells.[37]

LE-XRF Analysis: Cell Distribution and Colocalization of Co and Fe in Digestive Gland Cells. To confirm the data obtained with PIXE and gather information at the subcellular level, LE-XRF analyses were used to study colocalization of Co and Cu which was observed in all of the samples. Outside this region, Co was not detected. These results confirmed the absence of colocalization of Co and Fe, but Fe was found at some other locations (Figure 3A,B), indicating either the presence of Fe in the animals before the experiment or release of Fe from the particles. Since the concentrations of Fe analyzed by other methods (PIXE, AAS) did not show any increase of Fe in animals exposed to $CoFe_2O_4$ nanoparticles, we concluded that Fe is not derived in substantial amounts from $CoFe_2O_4$ nanoparticles.

AAS Analysis: Concentration of Co and Fe in Digestive Glands. After 14 days exposure of animals to $CoCl_2$ and $CoFe_2O_4$ NPs, the amounts of Co (experiments A and D) and Fe (experiment D) in digestive glands were measured. The amount of Co showed a statistically significant increase in both experiments in which animals were exposed to $CoCl_2$. This indicates that more Co accumulated when animals were exposed to Co ions as compared to nanoparticles. Statistically significant changes in experiment D occur among control animals and all exposed animals (Figure 4A). These results show that accumulation of Co in hepatopancreas is

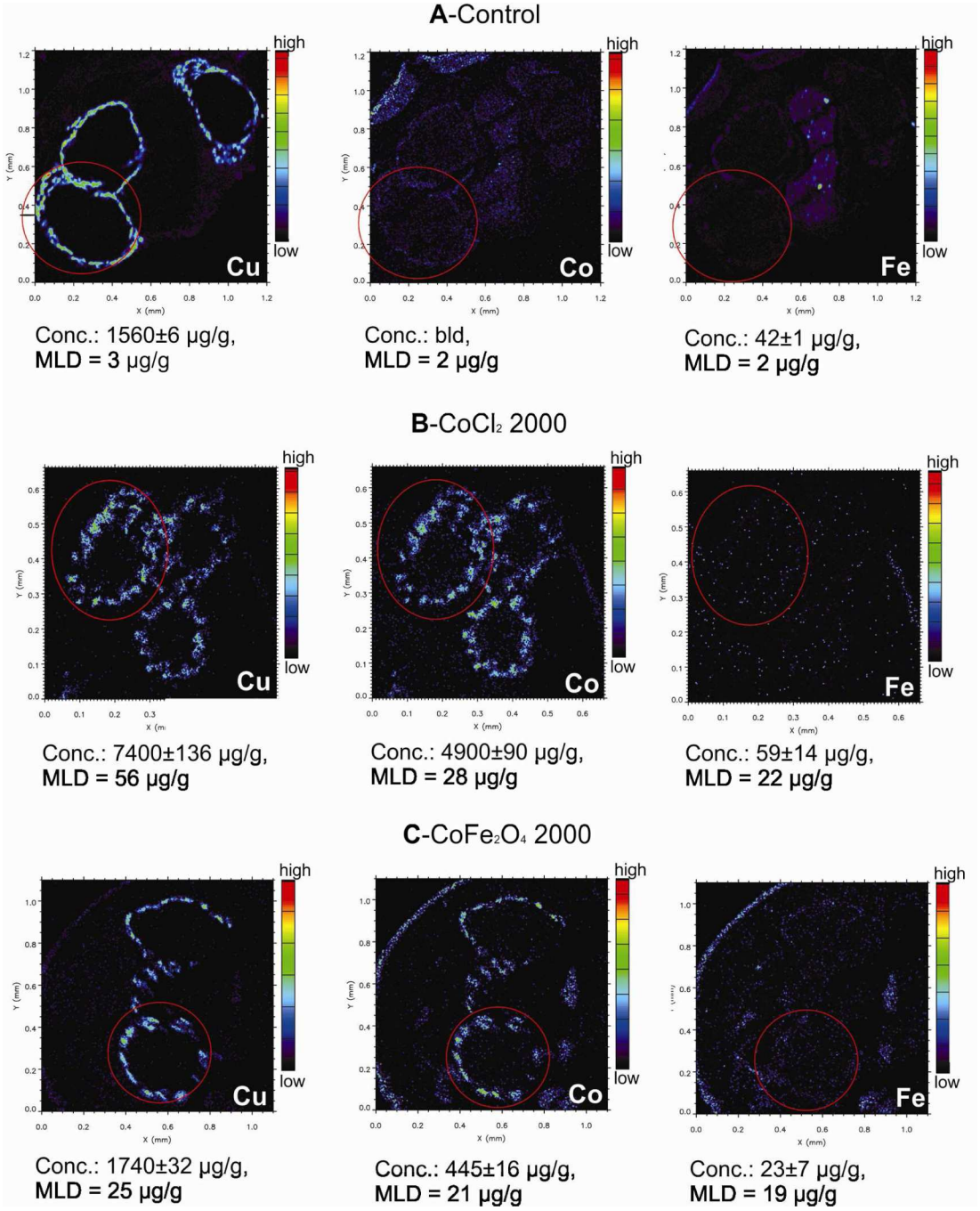

Figure 2. PIXE analyses of digestive gland cross section and corresponding concentrations of measured elements. (A) Elemental maps of Cu, Co, and Fe in digestive glands of a control animal. (B) Cross section of digestive glands of animal exposed to food dosed with 2000 μg $CoCl_2$/g dry mass of food. (C) Cross section of digestive glands of animal exposed to food dosed with 2000 μg nano-$CoFe_2O_4$/g dry mass of food.The elemental maps present the cross sections of three digestive gland tubes. Under each map, the concentrations of elements for selected encirculated glands are provided together with corresponding Minimum Limit of Detection (MLD).

dose-dependent. No Fe accumulation was detected when animals were fed $CoFe_2O_4$ nanoparticles (Figure 4B).

Concentration of Co and Fe in the Supernatant of the nano-$CoFe_2O_4$ Suspensions. It was expected that ultracentrifugation would cause sedimentation of nanoparticles; however, the possibility remains that some of the particles can be found in the supernatant. Therefore, the supernatant containing dissolved Co and Fe ions and actual particles was treated with 37% HCl (Merck) (0.5 M) according to Elzey and Grassian.[38] It was expected that if nanoparticles were present in the supernatant, acidification would increase the amount of Co and Fe ions. However, the concentrations of Co and Fe in the acidified and nonacidified part of the same supernatant did not differ; therefore, we conclude that the ultracentrifugation procedure efficiently removed the nanoparticles.

Centrifugation did not remove any ions from the $CoCl_2$ solution (Table S2 of the SI). After separation of the dissolved fraction of Co and Fe ions from $CoFe_2O_4$ NP suspensions by ultracentrifugation, the remaining metal content represented a very small proportion of the Co originally present (0.008% in

dx.doi.org/10.1021/es305132g | Environ. Sci. Technol. 2013, 47, 5400−5408

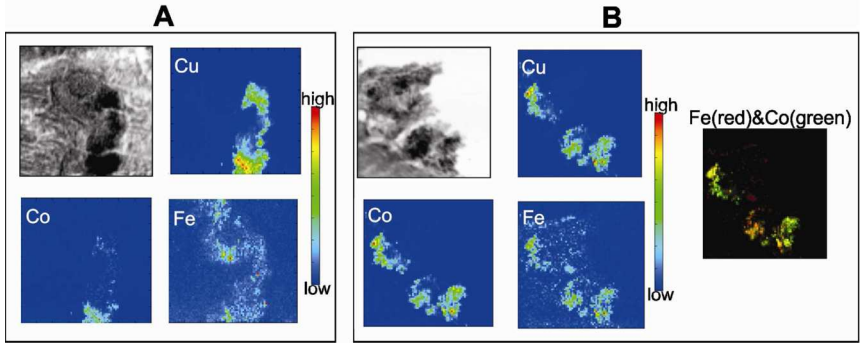

Figure 3. 80 × 80 μm^2 X-ray absorption images of part of digestive gland epithelium and the corresponding XRF maps. The distribution of Cu, Fe, and Co in control animal (A) and in animals fed with food dosed with 2000 μg nano-$CoFe_2O_4$/ g dry mass of food (B). The colocalization of Co and Cu and Co and Fe for the fed animal are shown in (B) as well. It is shown that Co and Fe do not colocalize. All images and XRF maps were collected using photon energy of 1.14 keV.

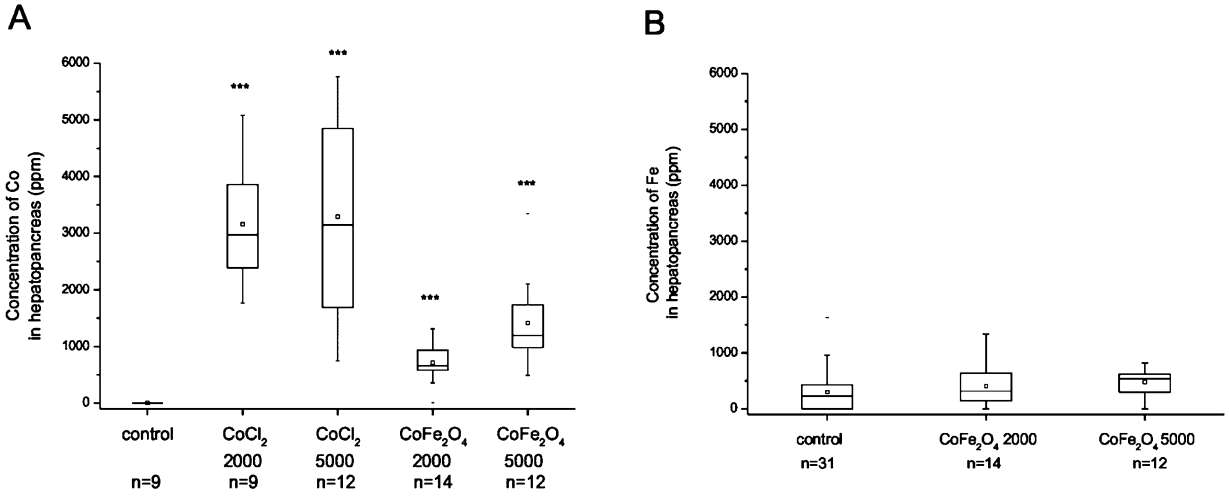

Figure 4. Concentration of Co or Fe in hepatopancreas after 14 days of feeding with $CoCl_2$ salts or nano-$CoFe_2O_4$ dosed food in experiment D, measured by AAS. (A) concentration of Co in hepatopancreas in experiment D. (B) Concentration of Fe in hepatopancreas in experiment D. Symbols on the box plot represent minimum and maximum data values (whiskers), mean value (□), 75th percentile (upper edge of box), 25th percentile (lower edge of box), median (line in box) and max and min value (−). Statistical differences between exposed and control animals are marked with *** ($p < 0.001$). Nominal exposure concentration (2000 or 5000 μg $CoCl_2$ or nano-$CoFe_2O_4$/g of leaf) and number of animals per group (n) are provided on x-axis. Ppm stands for unit μg/g.

the case of 2000 and below detection limit in the case of 5000 mg/L of Co in $CoFe_2O_4$ NP suspensions, respectively) and Fe (below detection limit in the case of 3826 and 9565 mg/L of Fe in $CoFe_2O_4$ NP suspensions, respectively). It is important to note that the actual concentration of Co and Fe ions quantified in the supernatants of ultracentrifuged $CoFe_2O_4$ NPs suspensions may also be smaller than the total concentration of Co and Fe quantified by AAS (comprising of Co and Fe ions and a small fraction of NPs that were not removed).

The recovery of original suspensions of $CoFe_2O_4$ NPs was 97−127%, in the limits of working error.

DISCUSSION

Feeding of the model terrestrial invertebrate *P. scaber* on food dosed with $CoFe_2O_4$ nanoparticles or Co ions (1000, 2000, or 5000 μg/g of leaf of $CoCl_2$ or nano-$CoFe_2O_4$) resulted in intracellular accumulation of Co ions, but not of particles. Toxic effects were ascribed to Co ions rather than $CoFe_2O_4$ nanoparticles themselves.

We have shown in our in vivo study that the observed toxicity as evidenced by reduced feeding rate and cytotoxicity as manifested by cell membrane stability are related to available metal ions in the food. The effect on feeding rate was dose-dependent while cell membrane destabilization was not significantly different between animals exposed to 1000 or 2000 μg/g of $CoCl_2$. This leads to the conclusion that if the amount of Co available in the food is high enough, it leads to cytotoxic effects. Available metal ions were inferred from the amount of accumulated Co^{2+} in the digestive gland cells and this amount was higher when animals were fed with food dosed with $CoCl_2$ than when fed food dosed with $CoFe_2O_4$ nanoparticles.

The digestive gland epithelium of the model organism did not internalize material by endocytosis, and consequently it was expected that ions will enter only through ion channels. However, in cases when cell membrane is destabilized, nanomaterials could enter the cells, but they are expected to be distributed throughout the cell. When metal ions enter the cells, they are transported to metal storing granules.[39] In our study, only digestive glands with nondestabilized membrane were selected for PIXE and LE-XRF elemental analyses. We have shown by X-ray-based techniques that only Co, but not Fe

dx.doi.org/10.1021/es305132g | Environ. Sci. Technol. 2013, 47, 5400−5408

entered cells. Cobalt was always found to be colocalized with Cu and this indicates that Co follows the same cellular pathways as other metal ions, such as Cu^{2+}, which are transported to metal storage granules where they accumulate. This suggests that only ions generated from $CoFe_2O_4$ nanoparticles or available from $CoCl_2$ salt are internalized and that Co^{2+} accumulation is dose-dependent.

Other authors report that Co nanoparticles and Co ions are both responsible for the effects on cells and explain that the nature of the effects depends on the type of the cell line, duration of exposure, and applied nanoparticle concentration.[15] Ponti et al.[40] reported that toxicity was higher for Co nanoparticles than for Co ions after 2 and 24 h exposure, while Papis et al. [14] showed that $CoCl_2$ has a more severe cytotoxic effect on human cell lines compared to Co_3O_4 nanoparticles.

Dissolution of metal ions and metal oxide nanoparticles has been studied in vitro in case of endocytosis[41,42] as well as in vivo with isopods (Golobič et al. 2012), rats,[43] and mice.[44] Dissolution of Co ions from nanoparticles has also been reported. Papis et al. [14] evaluated spontaneous dissolution of Co ions from Co_3O_4 NPs in phosphate buffered saline (PBS), distilled H_2O, and culture medium. Their results showed that release of Co^{2+} from NPs takes place in every tested medium but remains under 1% of the total Co in media. The percentage of leaching of Co ions from Co NPs in Dulbecco's Modified Eagle Medium (DMEM) was determined by Horev-Azaria et al.,[15] who found that incubation of the Co NPs for the 72 h resulted in decomposition of 44 ± 10% of the Co-NPs.

In our study, we also used ultracentrifugation to measure the release of Co from $CoFe_2O_4$ nanoparticles in distilled water. The level of Co in supernatants was found to very low (approximately 0.2 μg/mL for 2000 μg/mL of Co in $CoFe_2O_4$ nanoparticles and below the detection limit of AAS instrument for 5000 μg/mL of Co in $CoFe_2O_4$ nanoparticles). The animals assimilated an average of approximately 7% of consumed cobalt when fed with Co salts, and between 1% and 2% of cobalt when fed with cobalt nanoparticles. These data are not in agreement with the extremely low levels (from <0.009 μg/mL to 0.2 μg/mL) of dissolved Co indicated by the ultracentrifugation experiments. This finding suggests that the majority of assimilated Co decomposes inside the digestive system of tested animals and not in the suspension which was applied to the leaves. This is in agreement with our other studies on ZnO and CuCe (Drobne et al., unpublished).

The potential dissolution of particles inside organisms has not previously been intensively studied. More attention was given to chemical analytical methods for measuring dissolution of particles from suspensions in different suspensions. We propose the use of a model biological system with a terrestrial isopod for studying the potential dissolution of ions from metal-containing nanoparticles in biologically complex media. A system which allows measurement of dissolution of a variety of nanoparticles with different modifications is important to properly characterize particles before biomedical application, or for example, in the food industry.

■ ASSOCIATED CONTENT

Supporting Information

EDX spectra analyses of an abaxial leaf surface covered with a suspension of $CoFe_2O_4$ nanoparticles (nominal concentration 5000 μg/g); SEM characterization of $CoFe_2O_4$ nanoparticles and SEM/EDX analyses of $CoFe_2O_4$ nanoparticles on leaves from experiment D; SEM image of the surface of a leaf covered with $CoFe_2O_4$ nanoparticles; mass change of animals (mg) fed for 14 days on food dosed with $CoCl_2$ or $CoFe_2O_4$ nanoparticles; survival of animals fed for 14 days on food dosed with $CoCl_2$ or $CoFe_2O_4$ nanoparticles; and feeding rate (mg of consumed leaf per mg of animal mass) of animals fed for 14 days on food dosed with $CoCl_2$ or $CoFe_2O_4$ nanoparticles. This material is available free of charge via the Internet at http://pubs.acs.org.

■ AUTHOR INFORMATION

Corresponding Author

*Phone: + 386 1 423 33; fax: +386 1 257 33 90; e-mail: damjana.drobne@bf.uni-lj.si.

Notes

The authors declare no competing financial interest.

■ ACKNOWLEDGMENTS

Work of PhD student S.N. was supported by the Slovenian Research Agency within the framework of young researchers. Part of work was conducted within research projects financed by the Slovenian Research Agency (J1-4109) and within the seventh FP EU Project "NANOVALID" (Contract No. 263147). We thank G.W.A Milne for editorial assistance and Matej Hočevar from the Metals and Technology Institute, Ljubljana for scanning electron micrographs. We also thank FVG regional grant NANOTOX 0060-2009.

■ REFERENCES

(1) Zi, Z. F.; Sun, Y. P.; Zhu, X. B.; Yang, Z. R.; Dai, J. M.; Song, W. H. Synthesis and Magnetic Properties of $CoFe_2O_4$ Ferrite Nanoparticles. *J. Magn. Magn. Mater.* **2009**, *321*, 1251−1255.

(2) Baldi, G.; Bonacchi, D.; Innocenti, C.; Lorenzi, G.; Sangregorio, C. Cobalt Ferrite Nanoparticles: The Control of the Particle Size and Surface State and Their Effects on Magnetic Properties. *J. Magn. Magn. Mater.* **2007**, *311*, 10−16.

(3) Mornet, S.; Vasseur, S.; Grasset, F.; Veverka, P.; Goglio, G.; Demourgues, A.; Portier, J.; Pollert, E.; Duguet, E. Magnetic Nanoparticle Design for Medical Applications. *Prog. Solid State Chem.* **2006**, *34*, 237−247.

(4) Joshi, H. M.; Lin, Y. P.; Aslam, M.; Prasad, P. V.; Schultz-Sikma, E. A.; Edelman, R.; Meade, T.; Dravid, V. P. Effects of Shape and Size of Cobalt Ferrite Nanostructures on Their MRI Contrast and Thermal Activation. *J. Phys. Chem. C.* **2009**, *113*, 17761−17767.

(5) Arruebo, M.; Fernandez-Pacheco, R.; Ibarra, M. R.; Santamaria, J. Magnetic Nanoparticles for Drug Delivery. *Nano Today* **2007**, *2*, 22−32.

(6) Chemla, Y. R.; Crossman, H. L.; Poon, Y.; McDermott, R.; Stevens, R.; Alper, M. D.; Clarke, J. Ultrasensitive Magnetic Biosensor for Homogeneous Immunoassay. *Proc. Natl. Acad. Sci. U. S. A.* **2000**, *97*, 14268−14272.

(7) Hergt, R.; Dutz, S.; Muller, R.; Zeisberger, M. Magnetic Particle Hyperthermia: Nanoparticle Magnetism and Materials Development for Cancer Therapy. *J. Phys.: Condens. Matter.* **2006**, *18*, S2919−S2934.

(8) Salloum, M.; Ma, R. H.; Weeks, D.; Zhu, L. Controlling Nanoparticle Delivery in Magnetic Nanoparticle Hyperthermia for Cancer Treatment: Experimental Study in Agarose Gel. *Int. J. Hyperthermia* **2008**, *24*, 337−345.

(9) Zou, W. G.; Yan, M. D.; Xu, W. J.; Huo, H. R.; Sun, L. Y.; Zheng, Z. C.; Liu, X. Y. Cobalt Chloride Induces PC12 Cells Apoptosis through Reactive Oxygen Species and Accompanied by AP-1 Activation. *J. Neurosci. Res.* **2001**, *64*, 646−653.

(10) Petit, A.; Mwale, F.; Tkaczyk, C.; Antoniou, J.; Zukor, D. J.; Huk, O. L. Induction of Protein Oxidation by Cobalt and Chromium Ions in Human U937 Macrophages. *Biomaterials* **2005**, *26*, 4416−4422.

(11) De Boeck, M.; Lison, D.; Kirsch-Volders, M. Evaluation of the in Vitro Direct and Indirect Genotoxic Effects of Cobalt Compounds Using the Alkaline Comet Assay. Influence of Interdonor and Interexperimental Variability. *Carcinogenesis* **1998**, *19*, 2021−2029.
(12) Dokoumetzidis, A.; Macheras, P. a Century of Dissolution Research: From Noyes and Whitney to the Biopharmaceutics Classification System. *Int. J. Pharm.* **2006**, *321*, 1−11.
(13) Miao, A. J.; Zhang, X. Y.; Luo, Z. P.; Chen, C. S.; Chin, W. C.; Santschi, P. H.; Quigg, A. Zinc Oxide Engineered Nanoparticles Dissolution and Toxicity to Marine Phytoplankton. *Environ. Toxicol. Chem.* **2010**, *29*, 2814−2822.
(14) Papis, E.; Rossi, F.; Raspanti, M.; Dalle-Donne, I.; Colombo, G.; Milzani, A.; Bernardini, G.; Gornati, R. Engineered Cobalt Oxide Nanoparticles Readily Enter Cells. *Toxicol. Lett.* **2009**, *189*, 253−259.
(15) Horev-Azaria, L.; Kirkpatrick, C. J.; Korenstein, R.; Marche, P. N.; Maimon, O.; Ponti, J.; Romano, R.; Rossi, F.; Golla-Schindler, U.; Sommer, D.; Uboldi, C.; Unger, R. E.; Villiers, C. Predictive Toxicology of Cobalt Nanoparticles and Ions: Comparative In Vitro Study of Different Cellular Models Using Methods of Knowledge Discovery from Data. *Toxicol. Sci.* **2011**, *122*, 489−501.
(16) Zook, J. M.; Long, S. E.; Cleveland, D.; Geronimo, C. L. A.; MacCuspie, R. I. Measuring Silver Nanoparticle Dissolution in Complex Biological and Environmental Matrices Using UV-Visible Absorbance. *Anal. Bioanal. Chem.* **2011**, *401*, 1993−2002.
(17) Zimmer, M.; Topp, W. Homeostatic Responses in the Gut of *Porcellio scaber* (Isopoda: Oniscidea) Optimize Litter Degradation. *J. Comp. Physiol., B.* **1997**, *167*, 582−585.
(18) Zimmer, M.; Brune, A. Physiological Properties of the Gut Lumen of Terrestrial Isopods (Isopoda: Oniscidea): Adaptive to Digesting Lignocellulose? *J. Comp. Physiol., B.* **2005**, 275−283.
(19) Udovic, M.; Drobne, D.; Lestan, D. Bioaccumulation in *Porcellio scaber* (Crustacea, Isopoda) As a Measure of the EDTA Remediation Efficiency of Metal-Polluted Soil. *Environ. Pollut.* **2009**, *157*, 2822−2829.
(20) Pipan-Tkalec, Z.; Drobne, D.; Jemec, A.; Romih, T.; Zidar, P.; Bele, M. Zinc Bioaccumulation in a Terrestrial Invertebrate Fed a Diet Treated with Particulate ZnO or $ZnCl_2$ Solution. *Toxicology* **2010**, *269*, 198−203.
(21) Gyergyek, S.; Drofenik, M.; Makovec, D. Oleic-Acid-Coated $CoFe_2O_4$ Nanoparticles Synthesized by Co-Precipitation and Hydrothermal Synthesis. *Mater. Chem. Phys.* **2012**, *133*, 515−522.
(22) Valant, J.; Drobne, D.; Sepcic, K.; Jemec, A.; Kogej, K.; Kostanjsek, R. Hazardous Potential of Manufactured Nanoparticles Identified by in Vivo Assay. *J. Hazard. Mater.* **2009**, *171*, 160−165.
(23) McGahon, A. J.; Martin, S. J.; Bissonnette, R. P.; Mahboubi, A.; Shi, Y. F.; Mogil, R. J.; Nishioka, W. K.; Green, D. R. The End of the (Cell) Line—Methods for the Study of Apoptosis in Vitro. *Methods Cell Biol.* **1995**, *46*, 153−185.
(24) Vogel-Mikus, K.; Pelicon, P.; Vavpetic, P.; Krett, I.; Regvar, M. Elemental Analysis of Edible Grains by Micro-PIXE: Common Buckwheat Case Study. *Nucl. Instrum. Methods B* **2009**, *267*, 2884−2889.
(25) Schneider, T.; Strasser, O.; Gierth, M.; Scheloske, S.; Povh, B. Micro-PIXE Investigations of Apoplastic Iron in Freeze-Dried Root Cross-Sections of Soil Grown Barley. *Nucl. Instrum. Methods B* **2002**, *189*, 487−493.
(26) Vogel-Mikus, K.; Pongrac, P.; Kump, P.; Necemer, M.; Simcic, J.; Pelicon, P.; Budnar, M.; Povh, B.; Regvar, M. Localisation and Quantification of Elements within Seeds of Cd/Zn Hyperaccumulator *Thlaspi praecox* by Micro-PIXE. *Environ. Pollut.* **2007**, *147*, 50−59.
(27) Vogel-Mikus, K.; Regvar, M.; Mesjasz-Przybylowicz, J.; Przybylowicz, W. J.; Simcic, J.; Pelicon, P.; Budnar, M. Spatial Distribution of Cadmium in Leaves of Metal Hyperaccumulating *Thlaspi praecox* Using Micro-PIXE. *New Phytol.* **2008**, *179*, 712−721.
(28) Kaulich, B.; S., J.; David, C.; Di Fabrizio, E.; Morrison, G.; Charalambous, P.; et al. A European Twin X-ray Microscopy Station Commissioned at ELETTRA. *Proc. 8th Int. Conf. X-ray Microsc. Conf. Proc. Ser. IPAP.* **2006**, *7*, 22−25.
(29) Kaulich, B.; Thibault, P.; Gianoncelli, A.; Kiskinova, M. Transmission and Emission X-ray Microscopy: Operation Modes, Contrast Mechanisms and Applications. *J. Phys.: Condens. Matter.* **2011**, *23*, 8.
(30) Morrison, G. R.; A., G.; B., K.; D., B.; Kovac, a. J. A Fast-Readout CCD System for Configured-Detector Imaging in STXM. *Proc. 8th Int. Conf. X-ray Microsc. IPAP Conf. Ser.* **2006**, 377−379.
(31) Alberti, R.; Klatka, T.; Longoni, A.; Bacescu, D.; Marcello, A.; De Marco, A.; Gianoncelli, A.; Kaulich, B. Development of a low-energy x-ray fluorescence system with sub-micrometer spatial resolution. *X-Ray Spectrom.* **2009**, 205−209.
(32) Gianoncelli, A.; Kaulich, B.; Alberti, R.; Klatka, T.; Longoni, A.; de Marco, A.; Marcello, A.; Kiskinova, M. Simultaneous Soft X-ray Transmission and Emission Microscopy. *Nucl. Instrum. Methods Phys. Res., Sect. A* **2009**, *608*, 195−198.
(33) Sole, V. A.; Papillon, E.; Cotte, M.; Walter, P.; Susini, J. A Multiplatform Code for the Analysis of Energy-Dispersive X-ray Fluorescence Spectra. *Spectrochim. Acta, Part B.* **2007**, *62* (1), 63−68.
(34) Jorhem, L. Certified Reference Materials As a Quality Tool in Food Control: Much Used—Often Misused—Sometimes Abused. *Accredit. Qual. Assur.* **2004**, *9*, 305−310.
(35) Phillips, K. M.; Wolf, W. R.; Patterson, K. Y.; Sharpless, K. E.; Holden, J. M. Reference Materials to Evaluate Measurement Systems for the Nutrient Composition of Foods: Results from USDA's National Food and Nutrient Analysis Program (NFNAP). *Anal. Bioanal. Chem.* **2007**, *389*, 219−229.
(36) Golobič, M.; Jemec, A.; Drobne, D.; Romih, T.; Kasemets, K.; Kahru, A. Upon Exposure to Cu Nanoparticles, Accumulation of Copper in the Isopod *Porcellio scaber* Is Due to the Dissolved Cu Ions Inside the Digestive Tract. *Environ. Sci. Technol.* **2012**, *46*, 12112−12119.
(37) Marmorato, P.; Ceccone, G.; Gianoncelli, A.; Pascolo, L.; Ponti, J.; Rossi, F.; Salome, M.; Kaulich, B.; Kiskinova, M. Cellular Distribution and Degradation of Cobalt Ferrite Nanoparticles in Balb/3T3 Mouse Fibroblasts. *Toxicol. Lett.* **2011**, *207*, 128−136.
(38) Elzey, S.; Grassian, V. H. Nanoparticle Dissolution from the Particle Perspective: Insights from Particle Sizing Measurements. *Langmuir* **2010**, *26*, 12505−12508.
(39) Bibic, A.; Drobne, D.; Strus, J.; Byrne, A. R. Assimilation of zinc by *Porcellio scaber* (Isopoda, Crustacea) Exposed to Zinc. *Bull. Environ. Contam. Toxicol.* **1997**, *58*, 814−821.
(40) Ponti, J.; Colognato, R.; Franchini, F.; Gioria, S.; Simonelli, F.; Abbas, K.; Uboldi, C.; Kirkpatrick, C. J.; Holzwarth, U.; Rossi, F. A Quantitative in Vitro Approach to Study the Intracellular Fate of Gold Nanoparticles: From Synthesis to Cytotoxicity. *Nanotoxicology* **2009**, *3*, 296−306.
(41) Studer, A. M.; Limbach, L. K.; Van Duc, L.; Krumeich, F.; Athanassiou, E. K.; Gerber, L. C.; Moch, H.; Stark, W. J. Nanoparticle Cytotoxicity Depends on Intracellular Solubility: Comparison of Stabilized Copper Metal and Degradable Copper Oxide Nanoparticles. *Toxicol. Lett.* **2010**, *197*, 169−174.
(42) Brunner, T. J.; Wick, P.; Manser, P.; Spohn, P.; Grass, R. N.; Limbach, L. K.; Bruinink, A.; Stark, W. J. In Vitro Cytotoxicity of Oxide Nanoparticles: Comparison to Asbestos, Silica, And the Effect of Particle Solubility. *Environ. Sci. Technol.* **2006**, *40*, 4374−4381.
(43) Karabanovas, V.; Zakarevicius, E.; Sukackaite, A.; Streckyte, G.; Rotomskis, R. Examination of the Stability of Hydrophobic (CdSe)-ZnS Quantum Dots in the Digestive Tract of Rats. *Photochem. Photobiol. Sci.* **2008**, *7*, 725−729.
(44) Loginova, Y. F.; Kazachkina, N. I.; Zherdeva, V. V.; Rusanov, A. L.; Shirmanova, M. V.; Zagaynova, E. V.; Sergeeva, E. A.; Dezhurov, S. V.; Wakstein, M. S.; Savitsky, A. P. Biodistribution of Intact Fluorescent CdSe/CdS/ZnS Quantum Dots Coated by Mercaptopropionic Acid after Intravenous Injection into Mice. *J. Biophotonics* **2012**, *5*, 848−859.